ISSN 1674-1056
http://cpb.iphy.ac.cn
http://iopscience.iop.org/cpb
中国物理 B
Chinese Physics
中国物理
Chinese Physics B

Active hyperspectral imaging with a supercontinuum laser source in the dark

Zhongyuan Guo(郭中源), Yu Liu(刘煜), Xin Zheng(郑鑫), Ke Yin(殷科)

Citation: Chin. Phys. B . 2019, 28(3): 034206. **doi:** 10.1088/1674-1056/28/3/034206
Journal homepage: http://cpb.iphy.ac.cn; http://iopscience.iop.org/cpb

What follows is a list of articles you may be interested in

Nonlinear behavior of the population dynamics of three-level systems in the presence of single photon absorption

Allam Srinivasa Rao
Chin. Phys. B . 2019, 28(2): 024211. **doi:** 10.1088/1674-1056/28/2/024211

Laser absorption spectroscopy for high temperature H_2O time-history measurement at 2.55 μm during oxidation of hydrogen

Yu-Dan Gou(苟于单), De-Xiang Zhang(张德翔), Yi-Jun Wang(王易君), Chang-Hua Zhang(张昌华), Ping Li(李萍), Xiang-Yuan Li(李象远)
Chin. Phys. B . 2018, 27(7): 074213. **doi:** 10.1088/1674-1056/27/7/074213

Analysis of algebraic reconstruction technique for accurate imaging of gas temperature and concentration based on tunable diode laser absorption spectroscopy

Hui-Hui Xia(夏晖晖), Rui-Feng Kan(阚瑞峰), Jian-Guo Liu(刘建国), Zhen-Yu Xu(许振宇), Ya-Bai He(何亚柏)
Chin. Phys. B . 2016, 25(6): 064205. **doi:** 10.1088/1674-1056/25/6/064205

Lasing dynamics study by femtosecond time-resolved fluorescence non-collinear optical parametric amplification spectroscopy

Wei Dang(党伟), Qing Liao(廖清), Peng-Cheng Mao(毛鹏程), Hong-Bing Fu(付红兵), Yu-Xiang Weng(翁羽翔)
Chin. Phys. B . 2016, 25(5): 054207. **doi:** 10.1088/1674-1056/25/5/054207

Wavelength modulation spectroscopy at 1530.32 nm for measurements of acetylene based on Fabry-Perot tunable filter

Yun-Long Li(李运龙), Bing-Chu Yang(杨兵初), Xue-Mei Xu(许雪梅)
Chin. Phys. B . 2016, 25(2): 024208. **doi:** 10.1088/1674-1056/25/2/024208

Active hyperspectral imaging with a supercontinuum laser source in the dark*

Zhongyuan Guo(郭中源)[1], Yu Liu(刘煜)[2], Xin Zheng(郑鑫)[1], and Ke Yin(殷科)[1,3,†]

[1] *State Key Laboratory of High Performance Computing, College of Computer, National University of Defense Technology, Changsha* 401173, *China*
[2] *College of Advanced Interdisciplinary Studies, National University of Defense Technology, Changsha* 410073, *China*
[3] *National Innovation Institute of Defense Technology, Academy of Military Sciences of the People's Liberation Army of China, Beijing* 100071, *China*

(Received 19 September 2018; revised manuscript received 2 January 2019; published online 22 February 2019)

An active hyperspectral imaging (HSI) system was built with a supercontinuum (SC) laser illuminator and a visible/near-infrared hyperspectral camera, which was used for object spectrum detection in the dark. It was demonstrated that the Gaussian-like distribution of the SC illuminator can still be used for accurate reflectance spectrum measurement once the illuminator was characterized in advance. The validity of active HSI results was demonstrated by comparison with passive results. Then, the active HSI system was used to acquire reflectance spectra of different objects in just one push-broom measurement successfully. With algorithms of principal component analysis clustering and unsupervised *K*-means spectral classification, this active HSI system with high spectral and spatial resolutions was demonstrated to be efficient and applicable for specific spectrum detections.

Keywords: laser spectroscopy, active hyperspectral imaging, supercontinuum laser

PACS: 42.62.Fi, 02.70.Hm, 42.81.Wg **DOI:** 10.1088/1674-1056/28/3/034206

1. Introduction

The reflectance spectrum characteristics of objects are considered as one of the most important information to evaluate their physical and chemical properties.[1] Hyperspectral imaging (HSI) system combines the great advantages of both spectroscopy and tomography, with measured subtle variations in spectral reflectances, and can provide a means of classification and identification of objects that are normally, in standard three-color imagery, indistinguishable. However, traditional HSI is passive,[2] which only measures the reflected sun light from object surfaces and so is strictly limited to daytime when enough solar radiation exists. Under the conditions like the shadow, the traditional HSI system has difficulty to be effective since the illumination is insufficient.[3,4] What is more, in some extreme conditions where the sun light could not reach, such as in the dark, caves, or deep waters,[5] hyperspectral detection of objects is not possible by using the traditional way.

In recent years, the rapid development of unmanned platforms greatly extends the human perception.[6] These platforms usually require both passive and active sensing systems, such as lidar, micro-wave/millimeter-wave radar, sonar, and of course hyperspectral sensors.[7] Among these systems, active electro-optical sensing systems in the visible or infrared (VIS/IR) region enjoy many advantages over passive systems.[8] As for active HSI, a broadband light source[9] is the prerequisite. When compared to active HSI system illuminated by lamps, supercontinuum (SC) laser illuminator[10,11] can particularly not only increase the illumination brightness but also extend the work distance up to kilometers. With the transition from passive to active, HSI system can work day and night,[12] and has the ability to eliminate shadows.

Historically, the first active HSI system with a SC laser was put forward by MIT Lincoln Laboratory in 1999.[13] They demonstrated that the SC laser illumination offered HSI system great promise in concealed and obscured target detection. Besides, active HSI system has the advantages of determinate illumination parameters in advance. With either numerical or experimental methods, SC laser illumination conditions at arbitrary distances can be determined. By detecting the reflected broadband light from object surfaces, the spectral information of interest can be calculated out. But limited by the development of SC lasers, active HSI system has witnessed a slow development.[14–16] Most of the previous studies rarely concerned about the spatial characteristics of active HSI systems, although this parameter is critically important for accurate spectrum detections. Note that the Gaussian-like beam profiles of SC laser would make the illumination totally different from uniform lamps. Therefore, only adopting the average SC laser spectrum to retrieve the reflectance spectra is inappropriate.[12]

In this paper, an improved active HSI system with the consideration of the laser beam signature is presented. Section 2 describes the detailed experimental setup and methodology. Section 3.1 calibrates the SC laser illuminator by in-

*Project supported by the Opening Foundation of State Key Laboratory of High Performance Computing, China (Grant No. 201601-02), the Open Research Fund of Hunan Provincial Key Laboratory of High Energy Technology, China (Grant No. GNJGJS03), the Opening Foundation of State Key Laboratory of Laser Interaction with Matter, China (Grant No. SKLLIM1702), and the China Postdoctoral Innovation Science Foundation (Grant No. BX20180373).

†Corresponding author. E-mail: cqyinke@126.com

© 2019 Chinese Physical Society and IOP Publishing Ltd

vestigating its spatially-related spectra. Section 3.2 describes a formula for calculating the reflectance spectra with the presented active HSI measurement. The active HSI results are in good agreement with passive results by comparing their spectral characteristics. In Section 3.3, two more complicated conditions are built, one for principal component analysis (PCA) clustering and the other one for unsupervised spectral classification. Conclusions and prospects are made in Section 4. As a proof-of-principle study of accurate active HSI system, this work fulfills the technical requirements for specific spectrum detection applications.

2. Experimental setup and methodology

Figure 1(a) shows the schematic experimental setup. The active HSI system comprises a home-made SC laser source as the broadband coherent illuminator, and a commercial visible and near-infrared (VIS/NIR) hyperspectral camera (Zolix, GaiaField-F-V10) as the detection instrument. A computer program is used to control the spectrum measurement. The broadband SC laser has an average optical power of 4.5 W and a spectral range of 450–2400 nm at −20 dB level below the peak. The SC laser is compact with a size of 260×240×70 mm^3, driven by a direct current (DC) power supply. An achromatic doublets mounted on an *xyz* translation stage is used to transmit the SC laser to objects. Figure 1(b) shows the visible photo of the SC laser spot measured in the dark. The laser beam diameter on the plane of target is ∼ 20 cm.

In the experiments, a variety of different objects, including a white diffuse plate, green fresh leaves, plastics, a yellow carton, and a camouflage net, were put ∼ 5 m away from the active HSI system. In order to avoid the effect of ambient light, active HSI experiments were conducted in the dark (lights off). To eliminate the effect of angular reflectance distribution,[17] the camera position was fixed and put as close as possible to the SC laser beam. Basic specifications of the experimental setup are presented in Table 1. With these parameters, the spatial resolution of the hyperspectral camera is calculated to be ∼ 0.8 mm. Meanwhile, the spectral resolution of the camera is set to be 3.5 nm, which is less than 10 nm and high enough for identifying different materials.

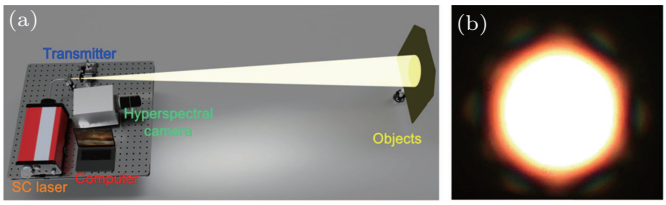


Fig. 1. Experimental setup. (a) Schematic illustration; (b) photo of SC laser spot.

The active HSI experiments were divided into three stages. In the first stage, the output SC laser was directly projected onto the white diffuse plate, and wavelength dependent SC beam profiles were measured to illustrate the non-uniform illumination. In the second stage, a formula was introduced to calculate the spatially-related reflectance of objects. Active HSI experiments with fresh leaves were implemented to demonstrate that the consideration of spatially-related reflectance was feasible. These measured active reflectance spectra were also compared to passive results, showing the advantage of active HSI measurement at the infrared region. In the last stage, two application conditions were built. PCA clustering and unsupervised spectral classification algorithms were used to show that active HSI results were efficient for further data analysis and information extraction.

Table 1. Basic specifications of experimental setup.

Setup	Parameters	Value	Setup	Parameters	Value
SC laser	Spectrum	450–2400 nm	Hyperspectral camera	Spectral range	400–1000 nm
	Average power	4.5 W		Spectral resolution	3.5 nm
	Repetition rate	170 kHz		Detector dimension	1392 × 1040
	Pulse duration	6 ns		Field of view	20°
	Output beam	LP01		Data bytes	16 bit
	Beam diameter	∼ 20 cm		Numerical aperture	F/2.8

3. Results and discussions

The experimental tests have been conducted according to the methodology described above. In this section, the corresponding experimental results are analyzed and discussed subsequently.

3.1. Calibration of SC laser illuminator

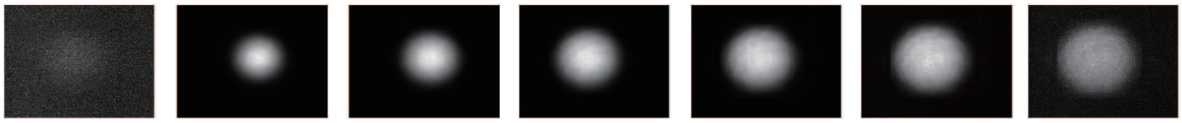
Before active HSI measurement, the SC laser illuminator is first characterized with a white diffusive plate. The results are depicted in Fig. 2. As shown in Fig. 2(a), beam profiles of the SC laser at different wavelengths are quite different. From left to right, the wavelengths are 400 nm, 500 nm, 600 nm, 700 nm, 800 nm, 900 nm, and 1000 nm, respectively. The reasons are that the divergence angles and beam waists of the SC laser increase as the wavelengths increase,[8] resulting in larger beam diameters at the longer wavelengths. The beam profile at 400 nm is blear because the SC light at 400 nm is too weak. Figure 2(b) shows the pseudo-colored SC laser spot image. Beam intensities at three wavelengths of 578.92 nm, 645.85 nm, and 758.75 nm are used. Along the vertical line

plotted in Fig. 2(b), spectra at 13 pixels equally-spaced from the beam center to edges are plotted in Fig. 2(c). Obviously, the measured illumination spectra are totally different from each other. The Savitzky–Golay method is adopted for denoising of the intensities.

The aforementioned results demonstrate that the SC laser has a non-uniform intensity distribution. So it is found that the formula used to calculate the reflectance spectrum with a spatially-independent spectrum $I(\lambda)$ is inappropriate. We suggest that the active SC laser illumination can be presented by a general intensity profile $I(x,y,\lambda)$ which considers the spatial distribution. For the validity, all object surfaces in this work are assumed to behave like Lambertian reflectors. Given these considerations, the reflectance spectra could be obtained with the following formula:

$$R(x,y,\lambda) = \frac{I_{\mathrm{D}}(x,y,\lambda) - I_{\mathrm{noise}}}{I_{\mathrm{SC}}(x,y,\lambda) - I_{\mathrm{noise}}} \times R_{\mathrm{plate}}(\lambda), \tag{1}$$

where $I_{\mathrm{D}}(x,y,\lambda)$ represents the measured hyperspectral intensity of interested objects, $I_{\mathrm{SC}}(x,y,\lambda)$ is the spatially-related illumination intensity of the white diffuse plate, I_{noise} is the measured camera noise in the dark (laser off), and $R_{\mathrm{plate}}(\lambda)$ is the reflectance spectrum of the white diffuse plate provided by the manufacturer. In the next section, we will prove that this formula is essential for increasing the detection accuracy of the active HSI system.



(a)

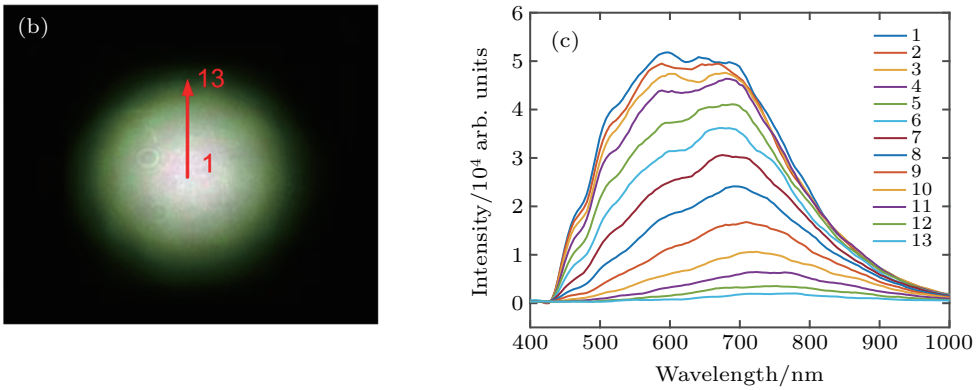


Fig. 2. Characteristics of SC laser illuminator. (a) Beam intensity profiles of SC laser at specific wavelengths; (b) pseudo-colored image of SC laser spot; (c) spectra at different pixels.

3.2. Hyperspectral reflectance measurement and analysis

For active hyperspectral reflectance measurement, green fresh leaves collected from a cinnamomun camphcra tree were used. Figure 3(a) shows the pseudo-colored image of the HSI result. As can be seen, the SC laser beam covers the most part of these leaves. For a better understanding, spectra at discrete 18 pixels in the yellow rectangle are used to calculate the reflectance spectra. Figure 3(b) plots the results. Note that the spectra below 450 nm should be neglected because the illumination light shorter than 450 nm is too weak. From Fig. 3(b), we can see that the calculated reflectances show typical spectral characteristics of green vegetation, like the small peaks from 520 nm to 600 nm, the steep red edges from 700 nm to 750 nm, and the infrared high reflectance regions from 750 nm to 1000 nm. The thick line in black is the average spectrum. For comparison, the average spectral intensity of the SC laser is used for the reflectance calculation and results are plotted in Fig. 3(c). Obviously, spectral variations in Fig. 3(b) are much smaller than that in Fig. 3(c). To quantify them, the standard deviations (STDs) of reflectance are calculated. We find that the STD at individual wavelength in Fig. 3(b) is about half of the STD in Fig. 3(c). These results illustrate that for the active HSI with SC laser illumination, it is necessary to consider the spatial distribution to ensure high accuracy.

Next, we prove the effectiveness of the improved active HSI system by comparing experimental results to passive HSI results. Figure 4 depicts the spectral characteristics of fresh leaves in a passive HSI measurement. The sun illumination spectrum is plotted in Fig. 4(a). Originated from the intrinsic black-body radiation, the sun illumination at the infrared region drops much faster than the SC laser. It is found that the illumination intensities with wavelengths longer than 900 nm are almost the same with the noise. Inevitably, the low signal to noise ratios bring inaccurate reflectance spectra. Figure 4(b) shows the retrieved passive hyperspectral reflectance. Obviously, when the wavelengths are shorter than 900 nm, there is a good consistency between the passive and active HSI measurements. But the passive reflectances lose their flatness in the infrared region where wavelengths are longer than 900 nm.

Therefore, it shows that an active HSI system illuminated by a SC laser with tailored spectrum has advantages when compared to passive HSI system and brings high detection accuracy.

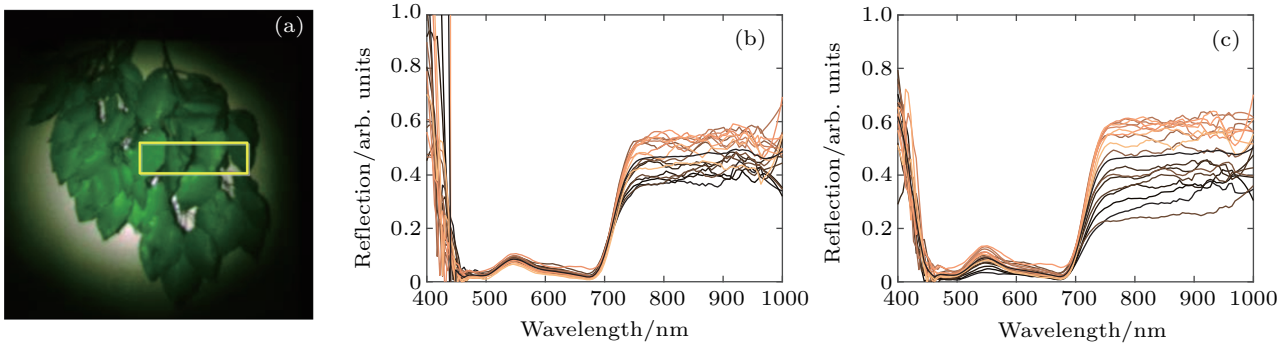


Fig. 3. Characteristics of fresh leaves. (a) Pseudo-colored image; (b) retrieved reflectance with spatially-related SC laser illumination; (c) retrieved reflectance with average SC laser illumination.

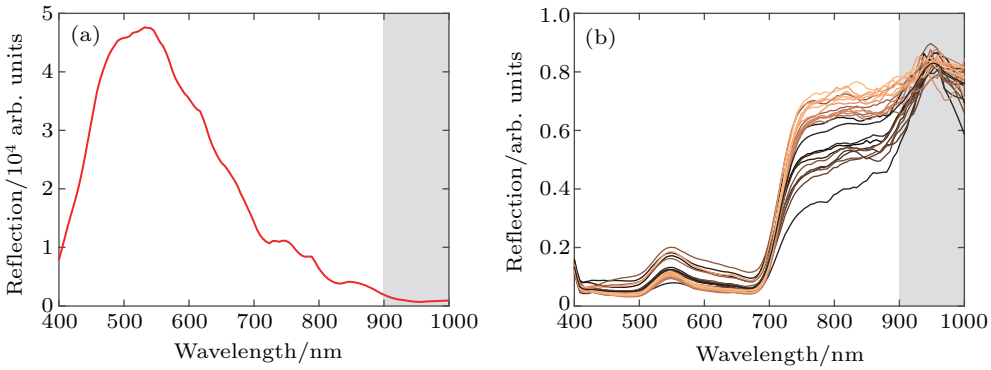


Fig. 4. Passive hyperspectral characteristics of fresh leaves. (a) Sun illumination; (b) reflectance spectra.

3.3. Applications of active HSI for complicated conditions

After the above work, a mixed scene is built including fresh leaves, plastic leaves, plastic flowers, and white vase. Different objects are located at different positions of the SC laser spot. As demonstrated above, the active HSI system is able to retrieve their reflectance with high accuracy. The results are shown in Fig. 5. Figure 5(a) depicts the pseudo-colored image of the measurement. There are four rectangles with red, blue, green, and pink colors, corresponding to green fresh leaves, plastic flowers, white vase, and plastic leaves, respectively. Retrieved reflectances in these rectangles are used for the following PCA clustering. Figure 5(b) plots the average spectra for each object. Clearly, different objects have their intrinsic spectral signatures. Reflectance spectra from 450 nm to 1000 nm are used for spectral analysis. The results from the PCAs are displayed in Fig. 5(c). As can be seen, the combination of PC1 (72.93%) and PC2 (22.07%) explains 95.00% of the total spectral variance. In this plot, object-specific points cluster closely together, indicating their consistent spectral signatures. Meanwhile, the 95% confidence intervals of the various objects are also depicted by ellipses. However, it is noted that ellipses for plastic flowers and white vase overlap with each other. This overlap can be interpreted as that the white vase and plastic flowers have similar NIR signatures as plotted in Fig. 5(b).

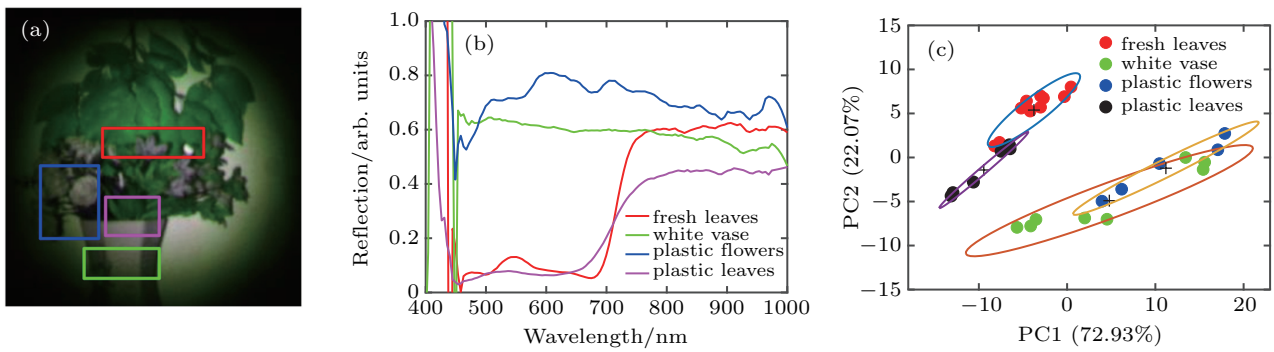


Fig. 5. PCA results. (a) Pseudo-colored image; (b) reflectance spectra of objects; (c) PCA plots of object results.

For actual applications, it is expected that the active HSI system can also be used to detect objects where passive HSI is unable to work. A concealed scene is built with a yellow carton covered by a camouflage net. The shadows would reduce the sun illumination even in the daytime. Therefore, passive HSI is very hard to identify the concealed carton.

In the experiments, the active HSI measurement has been conducted in the dark as well. Figure 6(a) shows the pseudo-colored image of the active HSI result. After retrieving the reflectance spectra, the data in the yellow square as shown in Fig. 6(a) is used for spectral classification analysis which has a dimension of 320×320×128. By removing the noise spectra below 450 nm, the final data dimension used for classification is 320×320×110. After that, an unsupervised *K*-means algorithm is used to perform the spectral classification. The number of classes is set to 2. Figure 6(b) shows the classification results. Obviously, the camouflage net and the yellow carton are successfully classified with pixel percentages of 68.87% and 31.13%, respectively. Note that the classification results at the four corners of the square are not correct. The reason is that the illumination at SC laser spot edges is too low to retrieve the accurate reflectance spectra. Figure 6(c) plots the measured spectra of the yellow carton and the camouflage net.

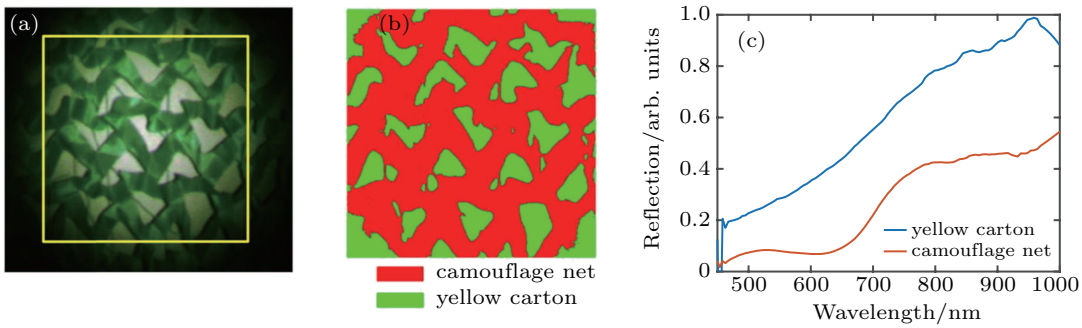


Fig. 6. Spectral classification results. (a) Pseudo-colored image; (b) classification results; (c) reflectance spectra of camouflage net and yellow carton.

4. Conclusion and perspectives

With the above demonstrations in this paper, one can see that with the active illumination to HSI system, high accurate spectral information of objects can be obtained. When compared to other laser-based spectral detections such as spectral lidar,[18] active HSI system provides much higher spatial and spectral resolutions. The hyperspectral data can be obtained in just one-time push-broom measurement, which is time-saving. We believe that the active HSI system consisting of a SC laser with higher illumination intensities and a hyperspectral camera with optimized parameters will performance much better in the future. Given that the short distance of this investigation, the influence of the atmosphere is not considered. However, when the work distance of active HSI system is increased to hundred meters, the atmospheric turbulence[19,20] and absorption should be considered.

To summarize, this work presents an active HSI system illuminated by a coherent SC laser. For the first time, the intensity profiles of SC laser for HSI detection have been considered. As demonstrated, this consideration increases the accuracy of detections by reducing the spectral STDs in half. The results show that the active HSI system has obvious advantages over passive HSI system. Two short standoff active hyperspectral measurements in the dark together with PCA clustering and spectral classification have been presented, indicating the possibility of active HSI system usage in future complicated conditions.

References

[1] Lin Z, Wang R, Wang Y, Wang L, Lu C, Liu Y, Zhang Z and Zhu L 2018 *Appl. Opt.* **57** D69
[2] Nischan M L, Joseph R M, Libby J C and Kerekes J P 2003 *Linc. Lab. J.* **14** 131
[3] Gronwall C, Steinvall O, Gohler B and Hamoir D 2016 *Appl. Opt.* **55** 5292
[4] Steinvall O, Elmqvist M, Chevalier T and Gustafsson O 2013 *Appl. Opt.* **52** 4763
[5] Odegard O, Mogstad A A, Johnsen G, Sorensen A J and Ludvigsen M 2018 *Appl. Opt.* **57** 3214
[6] Lejot J, Delacourt C, Piégay H, Fournier T, Trémélo M L and Allemand P 2007 *Earth Surf. Processes Landforms* **32** 1705
[7] Albert M, Teemu K R I, Tomi P, Scott B, Miika H and Toni L 2014 *Opt. Express* **22** 7172
[8] Ou Y, Zhang B, Yin K, Xu Z, Chen S and Hou J 2018 *Opt. Express* **26** 9822
[9] Skvortsov L A 2011 *Quant Electron.* **41** 1051
[10] Wang Y B, Hou J, Chen Z L, Chen S P, Song R, Li Y, Yang W Q and Lu Q S 2011 *Chin. Phys. Lett.* **28** 074208
[11] Chen H W, Jin A J, Chen S P, Hou J and Lu Q S 2013 *Chin. Phys. B* **22** 084205
[12] Islam M N, Freeman M J, Peterson L M, Ke K, Ifarraguerri A, Bailey C, Baxley F, Wager M, Absi A, Leonard J, Baker H and Rucci M 2016 *Appl. Opt.* **55** 1584
[13] Johnson B, Joseph R, Nischan M, AmyNewbury, Kerekes J, Barclay H, Willard B and Zayhowski J J 1999 *Proc. SPIE 3710, Detection and Remediation Technologies for Mines and Minelike Targets IV* August, 1999 Orlando, United States
[14] Kaasalainen S, Lindroos T and Hyyppa J 2007 *IEEE Geosci. Remote Sens. Lett.* **4** 211
[15] Orchard D A, Turner A J, Michaille L and Ridley K R 2008 *Proc. SPIE* **7115** 711506
[16] Hakala T, Suomalainen J, Kaasalainen S and Chen Y 2012 *Opt. Express* **20** 7119
[17] Hwang J 2014 *Appl. Opt.* **53** 6216
[18] Powers M A and Davis C C 2012 *Appl. Opt.* **51** 1468
[19] Ji X L 2010 *Acta Phys. Sin.* **59** 692 (in Chinese)
[20] Wang H, Wang X Z, Zeng A J and Yang K 2008 *Acta Phys. Sin.* **57** 634 (in Chinese)